Applied Thermal Engineering 126 (2017) 28–36

Contents lists available at ScienceDirect

Applied Thermal Engineering

journal homepage: www.elsevier.com/locate/apthermeng

Research Paper

Theoretical research on heterogeneous reduction of N_2O by char

Zhengyang Gao [a], Weijie Yang [a,*], Xunlei Ding [b], Yi Ding [a], Weiping Yan [a]

[a] School of Energy and Power Engineering, North China Electric Power University, Baoding 071003, China
[b] School of Mathematics and Physics, North China Electric Power University, Beijing 102206, China

HIGHLIGHTS

- The heterogeneous reduction mechanism of N_2O by char is revealed.
- Char provides free sites and reduces the energy barrier of N_2O reduction.
- The char edge structure has a notable influence on N_2O decomposition.
- The participation of CO can reduce activation energy of N_2O reduction.

GRAPHICAL ABSTRACT

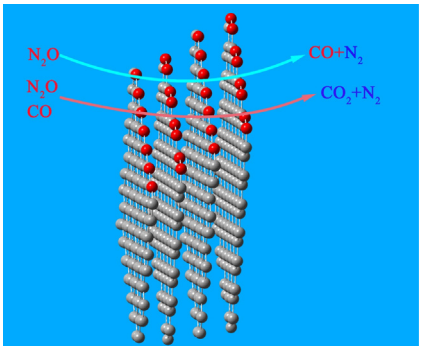

ARTICLE INFO

Article history:
Received 9 January 2017
Revised 17 April 2017
Accepted 21 July 2017
Available online 22 July 2017

Keywords:
N_2O
Heterogeneous reduction
Char
Thermodynamics
Kinetics

ABSTRACT

In order to investigate heterogeneous reduction of N_2O by char, quantum chemistry theoretical calculation based on zigzag and armchair char edge model was conducted. Thermodynamics and kinetics calculation were carried out combined with density functional theory (DFT) and conventional transition state theory (TST). Theoretical calculation results indicate that heterogeneous reduction of N_2O by char undergoes two stages: N_2O decomposition on char edge and residual oxygen desorption from char edge. N_2O decomposition process is an exothermic reaction and takes place spontaneously and irreversibly. Char acts as an important catalyst which not only provides free sites for the heterogeneous reduction but also reduces the reaction energy barrier. The participation of CO can significantly reduce reaction activation energy of residual oxygen desorption. The char edge structure has notable influence on activation energy of N_2O decomposition on char edge. Activation energy values of N_2O decomposition on zigzag and armchair char edge are 33.91 kJ/mol and 163.58 kJ/mol, respectively. The calculation results can not only deepen understanding of the reaction mechanism but also provide theoretical guidance for operation optimization of low N_2O emission.

1. Introduction

Nitrogen oxides (NO_x) emits from coal combustion is a major environmental pollutant, which can result in the greenhouse effect, the depletion of the ozone layer, the formation of acid rain and the generation of photochemical smog. Nitric oxide (N_2O) is a major pollutant of NO_x, particularly in circulating fluidized bed boiler (CFBB) [1]. N_2O emission from coal-fired CFBB is at range of 50–200ppmv [2], with an 0.2–0.4% growth rate every year.[3] Potential damage of N_2O to environment leads to an intense research on efficient removal of N_2O.

Extensive experimental studies on N_2O suggest that char and some metal oxides have strong N_2O reduction ability [4-13] and the reduction mainly derives from heterogeneous reactions [14]. Limestone ($CaCO_3$) addition to coal-fired boiler could contribute

* Corresponding author.
E-mail address: yangwj@ncepu.edu.cn (W. Yang).

http://dx.doi.org/10.1016/j.applthermaleng.2017.07.166
1359-4311/

to a decrease of N_2O emission, because limestone can promote the decomposition of N_2O [4]. Some metal oxides [5–8] (SiO_2, Al_2O_3, CaO, MgO and Fe_2O_3) in char and metal based zeolite [9,10] can also catalyze N_2O reduction, and N_2O reduction by metal oxides can be described as followings [11]:

$$N_2O \xrightarrow{catalyst} N_2 + 1/2O_2 \quad (R1)$$

Compared with metal oxides, char has more prominent effect on N_2O decomposition. Wang et al. [12] compared the effects of major metal oxides and fixed carbon in char on N_2O reduction and suggested that contribution of fixed carbon to N_2O reduction is superior to that of metal oxides. Char surface is relatively complex, but char active sites are mainly located at char edges. Kenshi Noda et al. [15] applied isotope gases to investigate the migration of nitrogen atom and concluded that carbon free sites can decompose N_2O into N_2 and residual oxygen adsorbed on char edge. The residual oxygen can react with char to generate CO. In detail, heterogeneous reduction of N_2O by char can be described as followings [15,16]:

$$N_2O + C() \rightarrow N_2 + CO \quad (R2)$$

Where C() is free active sites on char edge.

Furthermore, CO and temperature have a significant promotion effect on N_2O reduction by char.[11,12] Li et al. [11] studied the effect of temperature on N_2O reduction via changing the operating parameters and concluded that N_2O concentration can decrease from 90 mg/MJ to 40 mg/MJ when average temperature increases from 800 °C to 900 °C. Wang et al. [12] investigated the effect of CO on N_2O reduction applying synthetic coal and suggested that apparent activation energy of N_2O reduction decreases 21 kJ/mol with high concentration CO of 0.45%. Heterogeneous reduction of N_2O by char in the presence of CO can be expressed as followings [17]:

$$N_2O + CO \xrightarrow{char} N_2 + CO_2 \quad (R3)$$

In both cases, according to the reaction process, heterogeneous reduction of N_2O by char can be divided into two stages: N_2O decomposition on char edge and residual oxygen desorption from char edge [16].

Although heterogeneous reduction reaction of N_2O by char can be described by R2 and R3 briefly, the detailed reaction process of heterogeneous reduction of N_2O by char in molecular level still remains obscure [17]. Understanding the micro-mechanism of N_2O reduction can serve to optimize N_2O reduction and lower N_2O emissions. However, few theoretical calculations have been conducted to investigate heterogeneous reduction of N_2O by char. Therefore, a contribution from quantum chemistry calculations is obviously essential to elucidate this unclear mechanism.

Quantum chemistry is one of the most reliable methods to investigate the microscopic mechanism of chemical reaction [18–21]. Kyotani et al. [18] studied the adsorption configuration of N_2O on carbonaceous surfaces using an ab initio molecular orbital theory. Arenillas et al. [19] clarified the micro reaction path of NO reduction by char in density functional theory (DFT) of quantum chemistry. Zhang et al. [21] evaluated thermodynamic and kinetic of the reduction reaction between NO and char nitrogen by DFT theoretical calculation and revealed the micro-mechanism between NO and char nitrogen. Therefore, theoretical calculation study on heterogeneous reduction of N_2O by char via quantum chemistry method is reasonable and imperative.

In this study, we focus on microscopic reaction pathways, energy barriers, thermodynamic and kinetic analysis by a combination of DFT and conventional transition state theory (TST). In addition, the microscopic mechanism of CO on N_2O heterogeneous reduction by char is also investigated. The elementary reaction in this study can be expressed as followings:

$$N_2O + C() \rightarrow N_2 + C(O) \quad (R4)$$

$$C(O) \rightarrow Cd + CO \quad (R5)$$

$$CO + C(O) \rightarrow CO_2 + C() \quad (R6)$$

where C(O) and Cd are surface oxygen species and defect in char edge, respectively. To the best of the author's knowledge, this is the first theoretical research on heterogeneous reduction of N_2O by char. The calculation results can not only clarify microscopic reaction process and provide necessary kinetic parameters for operation optimization of low N_2O emission, but also reveal the microscopic mechanism of CO on N_2O heterogeneous reduction by char.

2. Computational details

2.1. Choice of char edge model

Reasonably simplified char edge model is a critical factor for substantially accurate results [20]. According to the previous theoretical results, we can know that armchair and zigzag benzene rings are two typical research models of carbonaceous surfaces [22]. Chen and Yang [23,24] investigated the chemical properties of graphene models by quantum chemistry calculation and suggested that seven zigzag and six armchair benzene rings are suitable models for reaction mechanism research owing to parameters in excellent agreement with experimental data. In addition, many reaction mechanisms involving carbonaceous surfaces have been successfully investigated employing these two char edge models [25–27]. Therefore, it is reasonable to select six armchair and seven zigzag benzene rings as char edge models, as shown in Fig. 1.

2.2. Choice of calculation method

Calculation method and basis set are directly related to the accuracy of calculation results and the computational time, which are other important factors in quantum chemistry calculations. Geometry optimizations of reactants, intermediates (IM), transition states (TS) and products were performed at B3LYP/6-31G(d) level, and single point energy calculations for thermodynamic analysis were conducted at B2PLYP theory (double hybrid density functional) with Def2-tzvp level (all electron basis sets for the first four row elements) so as to obtain accuracy energy barrier value. Previous studies have shown that B3LYP/6-31G(d) not only can obtain a good calculation accuracy but also can reduce calculation time in chemical reaction calculation [28–31]. In terms of spin multiplicity effect, the lowest energy states determined from single point energy calculations at B3LYP/6-31G(d) level for several spin multiplicities [32]. In addition, frequency calculations were completed to check imaginary frequency and obtain zero point correction [26]. Furthermore, intrinsic reaction coordinate (IRC) calculations were conducted to confirm the right connection between each TS and corresponding IM. All quantum chemistry calculations were performed at Gaussian09 software package [33].

Kinetic analysis of each reaction step was performed from 800 K to 1400 K by conventional TST [34], the equation is as following:

$$k^{TST} = \Gamma \times \frac{k_B T}{h} \times \frac{Q_{TS}}{Q_A Q_B} \times \exp\left(\frac{-E_b}{RT}\right) \quad (1)$$

where E_b is energy barrier of each reaction step, kJ mol^{-1}; R is universal gas constant, J mol^{-1} K^{-1}; T is reaction temperature, K; k_B is Boltzmann constant, J K^{-1}; h is Planck constant, J s; Q_{TS}, Q_A and Q_B are partial function of transition state *TS*, reactant *A* and reactant *B*,

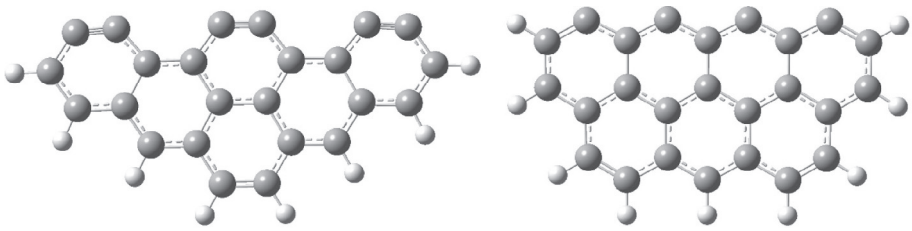

(a) Armchair char edge model (b) Zigzag char edge model

Fig. 1. char edge models.

respectively; Γ is quantum tunneling correction factor, which can be calculated by following equation:

$$\Gamma = 1 + \left(\frac{1}{24}\right) \times \left(\frac{h\upsilon_m c}{k_B T}\right)^2 \quad (2)$$

where υ_m is the imaginary frequency of transition states, cm^{-1}; c is light speed, m s^{-1}.

Equilibrium constant can be acquired through the following equation [35]:

$$\Delta G = G_B - G_A = -RT \ln K \quad (3)$$

where G_A and G_B are Gibbs free energy of reactants and products, kJ K^{-1}; K is equilibrium constant.

3. Results and discussion

In this section, heterogeneous reductions of N_2O based on armchair and zigzag char edge models are calculated and discussed respectively. The first step of heterogeneous reduction is the adsorption process of gases on char edge, gas concentration has an important effect on the competitive adsorption process of gas at char edges. However, understanding the reaction mechanism between gases adsorbed on char edge and char edge is the main goal of this study. Therefore, the gas concentration effect on heterogeneous reductions of N_2O is not considered in this work. In each char edge model, different adsorption configurations of N_2O on carbonaceous surfaces are considered and the most stable adsorption configuration is chosen to study heterogeneous reductions of N_2O. Furthermore, heterogeneous reduction of N_2O is divided into two stages to analyze, the stage of N_2O decomposition and the stage of residual oxygen desorption. In detail, the stage of residual oxygen desorption has two different situations depending on whether there is CO.

3.1. N_2O reduction on armchair char edge model

Optimized structures of reactants, products, IM, and TS in heterogeneous reduction of N_2O by char are shown in Fig. 2, and corresponding reaction potential energy surfaces are schematic in Fig. 3. In addition, imaginary frequency value, vibration direction, Mulliken atomic charge and bond length are given in Fig. 2.

3.1.1. N_2O decomposition on armchair char edge

As shown in Fig. 3, the stage of N_2O decomposition on char edge undergoes three transition states, and N_2 is separated from char edge with residual oxygen on char edge. Molecular structures in the reaction process can be obtained in Fig. 2. Firstly, N_2O molecular attack carbon free sites on the char edge, and N_2O adsorbs on char edge with the decrease of distance between N_2O and char edge. N_2O adsorption on char edge is a lower energy barrier (38.42 kJ/mol) and high exothermic (314.23 kJ/mol) step. Secondly, with N—O bond length increasing, N_2O decomposes into N_2 and oxygen atom adsorbed on char edge (1.497 Å(IM1) → 2.063 Å(TS2) → 3.201 Å(IM2)), which is almost barrier less (9.20 kJ/mol). Finally, N_2 desorption from char edge occurs is a higher-barrier(151.90 kJ/mol) step, with N—C(2) bond length increasing (1.324 Å(IM2) → 2.407 Å(TS3) → 3.658 Å(IM3)).

3.1.2. Oxygen desorption from armchair char edge

As described in Fig. 3, residual oxygen combines with CO in fuel gas into CO_2 is presented as red lines, and residual oxygen reacts with char edge into CO is expressed as blue lines. In the presence of CO, CO molecule adsorbs on char(O) surface with a large exothermic (164.84 kJ/mol) firstly, and adsorption configuration is similar to the structure of CO_2 adsorption on char edge [36]. Subsequently, residual oxygen combined with CO desorbs from char edge with a medium energy barrier (147.96 kJ/mol), and C—O bond length gradually extends in the desorption process can be seen in Fig. 2.

In the absence of CO, a novel reaction route for residual oxygen desorption from char edge is proposed in armchair char edge, as illustrated in Fig. 2. Firstly, residual oxygen reacts with carbon free sites in char edge into CO molecule through a small energy barrier (30.99 kJ/mol), and char edge deforms from hexagonal into pentagon in this process. Secondly, CO desorption from char edge occurs with a very high energy barrier (306.00 kJ/mol), forming a deformed char edge model (named as Cd1). This CO desorption process is available to accomplish under high temperature environment such as circulating fluidized bed. It is remarkable that ground state of armchair char edge model is singlet while that of Cd1 is triplet. In addition, Mulliken atomic charge of Cd1 is presented in Fig. 2. From Mulliken atomic charge of Cd1, C(2) in the middle of Cd1 contains bigger charge value compared with other carbon atoms in both sides, which may indicate that C(2) has higher reaction activity.

Comparing energy barrier value of two different oxygen desorption routes, residual oxygen desorption with CO is more likely to occur, which reveals that CO in flue gas favors residual oxygen desorption. According to energy barrier value of reaction steps, reaction rate-determining step can be identified. Rate-determining step of N_2O decomposition, which is N_2 desorption from char edge, is from IM2 to IM3. For residual oxygen desorption from char edge, rate-determining steps are from IM7 to IM8 (with CO) and from IM10 to IM11 (without CO), respectively.

3.2. N_2O reduction on zigzag char edge model

Optimized structures of N_2O heterogeneous reduction on zigzag char edge model are shown in Fig. 4, and corresponding reaction potential energy surfaces are schematic in Fig. 5. In addition, imaginary frequency value, vibration direction, Mulliken atomic charge and bond length are given in Fig. 4. Similar to N_2O reduction on armchair char model, heterogeneous reduction includes two stages, N_2O reduction on char edge and oxygen desorption from char edge, which are discussed particularly in this section.

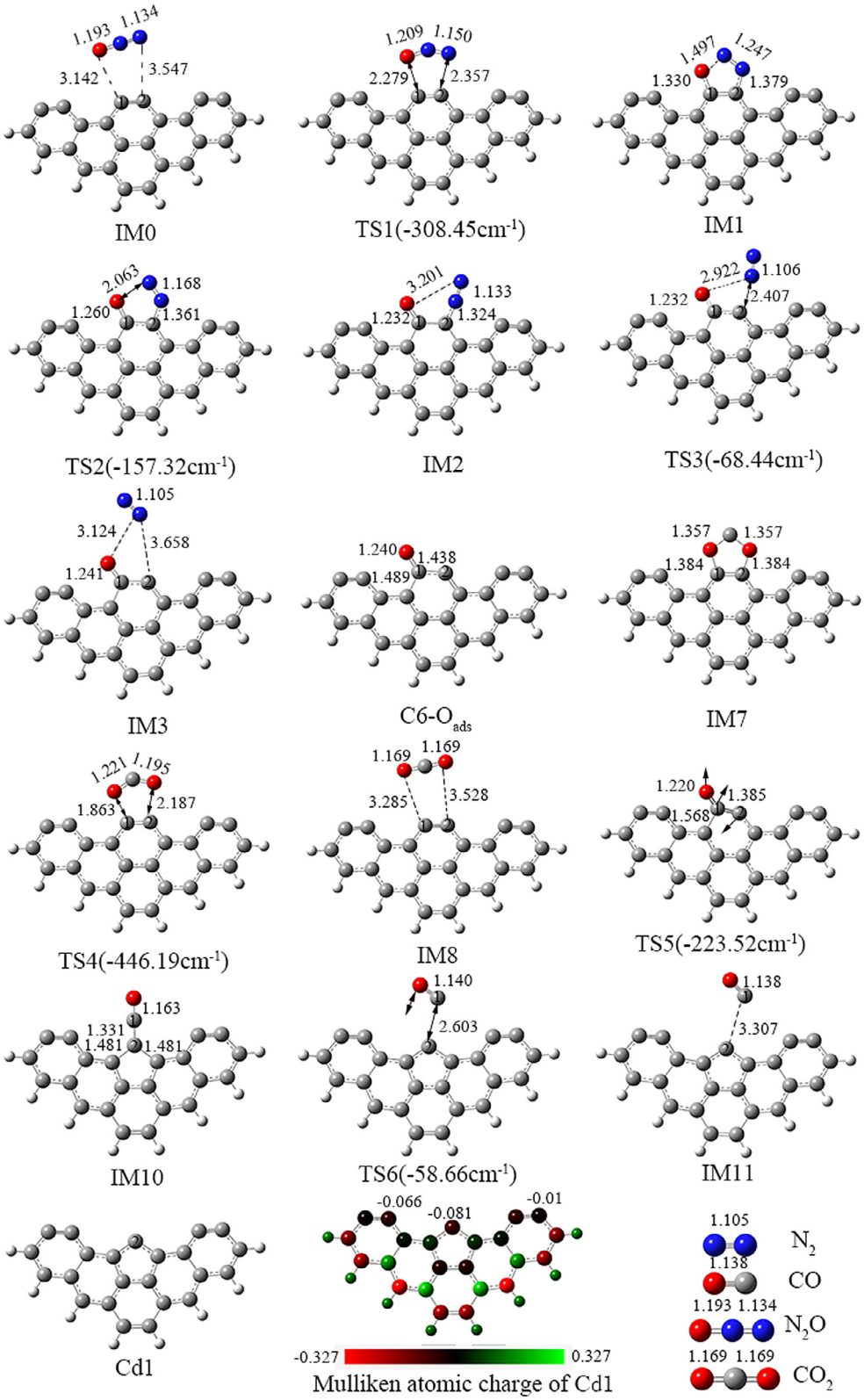

Fig. 2. Optimized structures of stable stationary points for N_2O reduction on armchair model. Bond lengths in Angstroms. (1 Å = 10^{-10} m).

3.2.1. N_2O decomposition on zigzag char edge

From Fig. 5, the stage of N_2O decomposition on char edge occurs via three transition states. Firstly, N_2O molecule adsorbs on char edge with a large exothermic (-403.35 kJ/mol). Comparing N—O bond length of N_2O molecule and N_2O adsorbed on zigzag char edge(1.193 Å vs 1.508 Å), N_2O adsorption on zigzag char edge belongs to dissociative adsorption, which is similar to CO_2 and HgCl adsorption on zigzag char edge [37,38]. Secondly, with N—O bond length increasing, N_2O decomposes into N_2 and residual oxygen adsorbed on char edge (1.508 Å(IM0) → 1.830 Å(TS1) → 3.063 Å(IM1)), which is a small energy barrier (27.53 kJ/mol). Thirdly, N_2 adsorbed on char edge undergoes a minor deformation

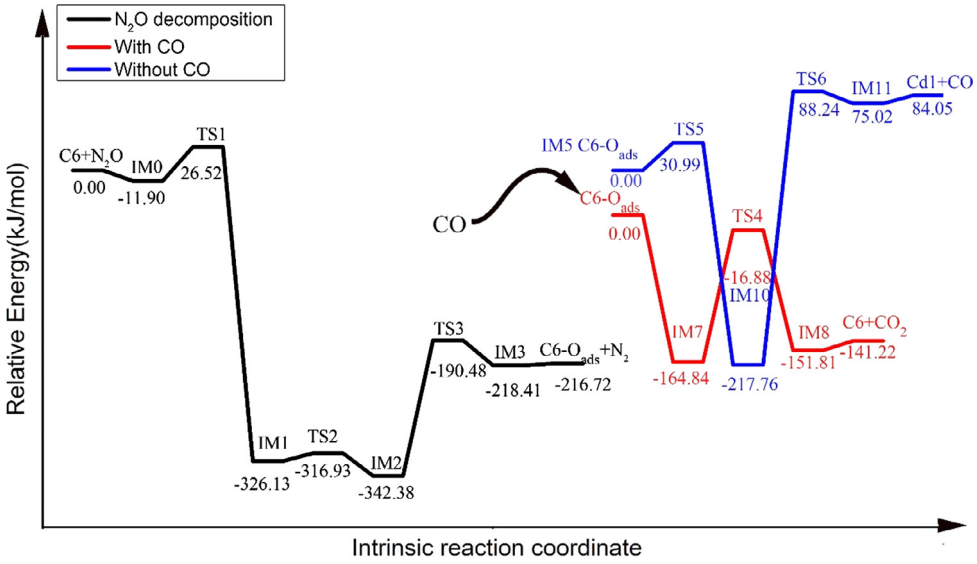

Fig. 3. Potential energy surfaces for N_2O reduction on armchair model.

via a small energy barrier (26.88 kJ/mol) while N—N bond and C—N bond are slightly stretched owing to activation of char edge (N—N:1.146 Å(IM0) → 1.164 Å(TS1) → 1.181 Å(IM1), C—N:1.340 (IM0) → 1.385 Å(TS1) → 1.440 Å(IM1)). Finally, N_2 desorption from char edge occurs with N—C bond length stretching (1.440 Å(IM1) → 1.871Å(TS2) → 3.614 Å(IM2)), which is a lower energy barrier (39.94 kJ/mol) step.

3.2.2. Oxygen desorption from zigzag char edge

Similar to armchair model, oxygen desorption from char edge is classified into two different situations depending on whether CO exists. Residual oxygen desorption with CO is presented in green lines, while this desorption process without CO is described as blue and red lines. It is noteworthy that spin multiplicity also has significant influence on residual oxygen desorption stage in the absence of CO.

In the presence of CO, CO molecule adsorbs on char(O) surface, and this adsorption configuration is the same to CO_2 adsorption on zigzag char edge.[37] Subsequently, with the dihedral angle of CO and char edge increasing (0°(IM11) → 44.43°(TS6) → 108.48°(IM12)), oxygen atom (O2) desorbs from char edge with a medium energy barrier (181.38 kJ/mol). Finally, desorption of CO_2 and char edge occurs via a 193.81 kJ/mol energy barrier, with O1—C3 bond length increasing (1.413 Å(IM12) → 1.839 Å(TS7) → 3.502 Å(IM13)).

In the absence of CO, two different spin multiplicity reactions experience only one transition state to complete residual oxygen desorption. Residual oxygen react with carbon atom in char edge surface into CO and defect char edge (Cd2) through a high energy barrier (245.32 kJ/mol) in two spin multiplicity reaction, while similar reaction undergoes a higher energy barrier (364.39 kJ/mol) to generate CO and another defect char edge (Cd3) in four spin multiplicity reaction. Comparing two different spin multiplicity reaction energy barrier values, two spin multiplicity reaction is more likely to occur. In addition, Mulliken atomic charge of two kinds defect char edges are presented in Fig. 4.

Analyzing heterogeneous reduction of N_2O by char, char plays a catalytic role and provides reaction sites for N_2O and CO in the presence of CO, while char react with residual oxygen into "defect char" and CO in the absence of CO. According to energy barrier value of reaction steps, reaction rate-determining step can be identified. Rate-determining step of N_2O decomposition is from IM2 to IM3, which is N_2 desorption from char edge. For oxygen desorption from char edge, rate-determining steps are from IM12 to IM13 (with CO), from IM5 to IM6 (without CO, spin = 2) and from IM5 to IM8 (without CO, spin = 4), respectively. Furthermore, comparing energy barrier magnitude of three different oxygen desorption routes, residual oxygen desorption with CO is more likely to occur which reveals that CO in flue gas favors residual oxygen desorption, revealing the microscopic mechanism of CO prompting the N_2O reduction in experiment [12].

Comparing N_2O decomposition on the two kinds of char edges, rate-determining steps are all N_2 desorption from char edge, indicating that N_2 desorption step is the key factor affecting reduction rate. Therefore, in order to acquire more thermodynamic information about this key stage, thermodynamic calculation of N_2O decomposition is performed in the Section 3.2. Additionally, kinetic analysis of each rate-determining steps is also conducted in the Section 3.3 so as to obtain kinetic parameters, such as pre-exponential factor and activation energy.

3.3. Thermodynamic of N_2O decomposition

Bed temperature is maintained between 950 and 1250 K with coal as fluidized bed material,[3] so thermodynamic parameters of N_2O decomposition are calculated at temperature range of 800–1400 K. Thermodynamic parameters such as enthalpy, entropy, Gibbs free energy and equilibrium constant are favor to understand reaction property, as shown in Table 1.

As illustrated in Table 1, enthalpy ΔH of N_2O decomposition on two char edge models at different temperatures are below zero, confirming that N_2O decomposition process is an exothermic reaction. In detail, N_2O decomposition on zigzag char edge model emits more thermal energy compared with armchair char edge model, and exothermic magnitude is about 470 kJ/mol. Gibbs free energy $\triangle G$ of N_2O decomposition on two char edge models at different temperatures are below zero, revealing that N_2O decomposition process can happen spontaneously at research temperatures. Moreover, equilibrium constants of N_2O decomposition on two char edge models at different temperatures are all higher than 10^5, suggesting that N_2O decomposition process can be carried out completely and take place irreversibly.

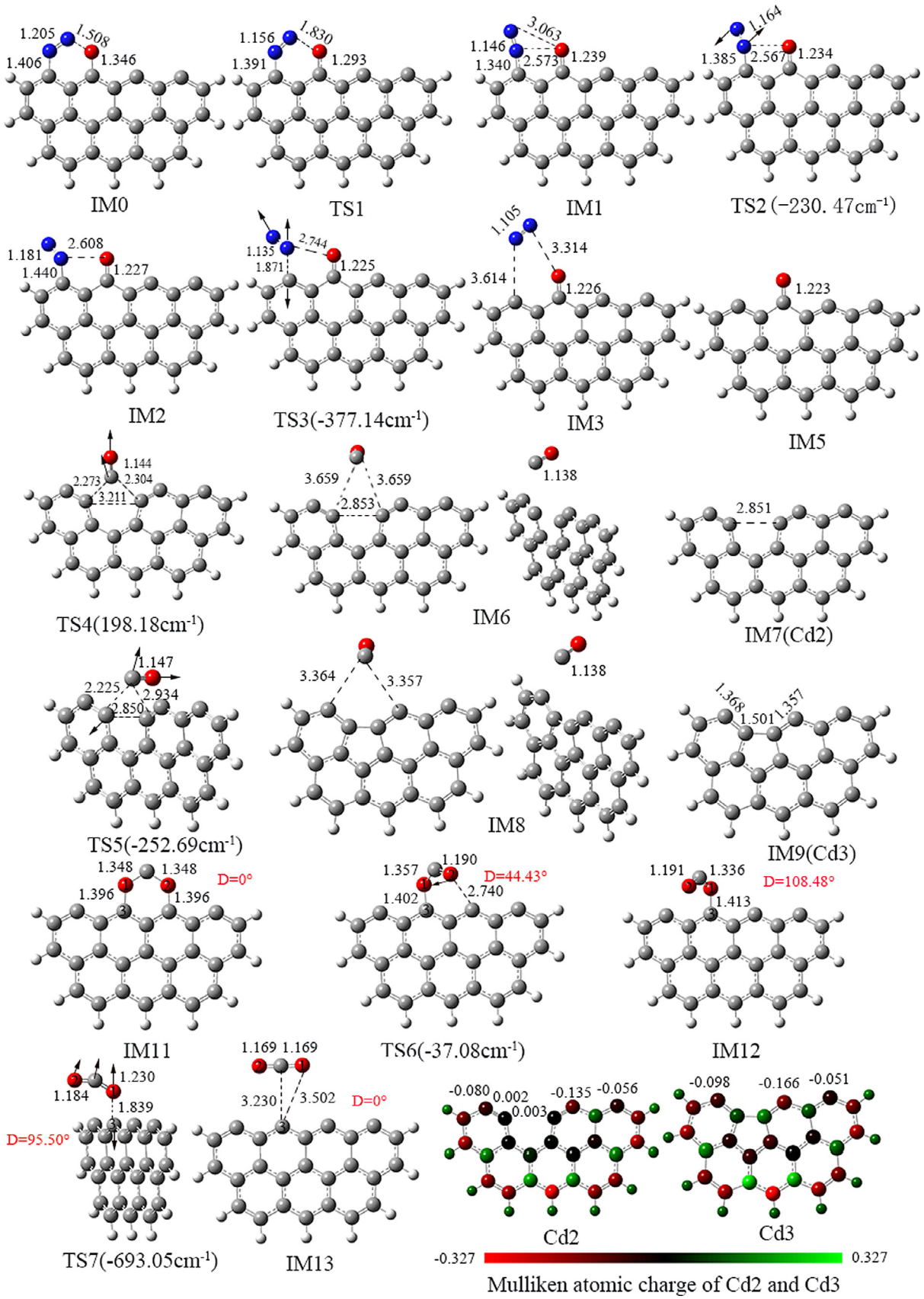

Fig. 4. Optimized structures of stable stationary points for N_2O reduction on zigzag model. Bond lengths in Angstroms.

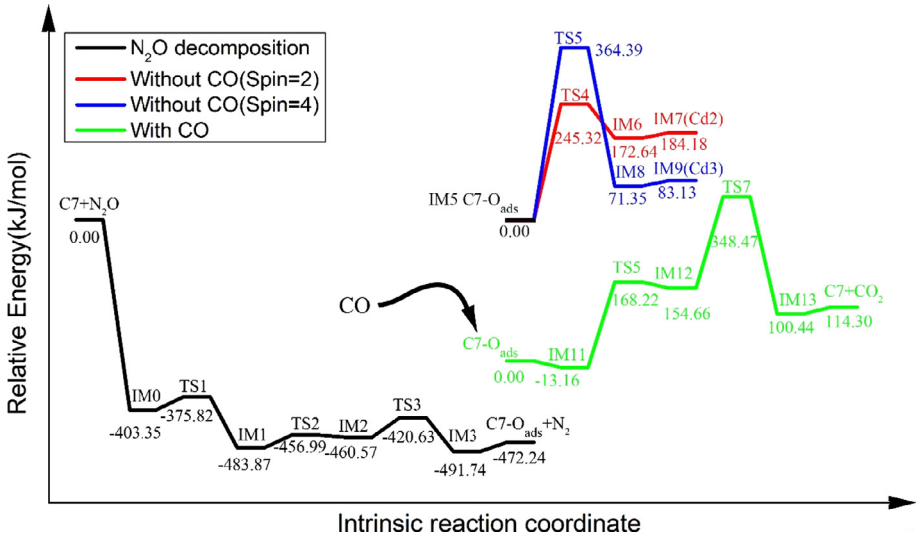

Fig. 5. Potential energy surfaces for N_2O reduction on zigzag model.

Table 1
Thermodynamic parameters at different temperatures.

Temperature (K)	C6-Armchair				C7-Zigzag			
	△H (kJ·mol^{-1})	△S (J·mol^{-1}·K^{-1})	△G (kJ·mol^{-1})	K	△H (kJ·mol^{-1})	△S (J·mol^{-1}·K^{-1})	△G (kJ·mol^{-1})	K
800	−205.84	−0.71	−205.18	2.50×10^{13}	−470.91	−6.68	−465.58	2.52×10^{30}
900	−205.66	−0.50	−205.12	8.03×10^{11}	−471.08	−6.88	−464.91	9.63×10^{26}
1000	−205.50	−0.33	−205.08	5.15×10^{10}	−471.25	−7.06	−464.21	1.77×10^{24}
1100	−205.35	−0.19	−205.05	5.46×10^{09}	−471.41	−7.21	−463.49	1.02×10^{22}
1200	−205.22	−0.08	−205.04	8.42×10^{08}	−471.56	−7.34	−462.77	1.40×10^{20}
1300	−205.10	0.02	−205.03	1.73×10^{08}	−471.69	−7.44	−462.03	3.67×10^{18}
1400	−204.99	0.10	−205.04	4.47×10^{07}	−471.81	−7.54	−461.28	1.63×10^{17}

3.4. Kinetics of the reaction between N_2O and char

Kinetics analysis can acquire reaction rate constant and lay the foundation for prediction model. According to Eqs. (1) and (2), the calculated reaction rate constants of rate-determining steps are plotted in Fig. 6, and rate constants based on armchair and zigzag char edge surface models are plotted with solid lines and dotted lines, respectively. Besides, corresponding Arrhenius parameters acquired from fitting the reaction rate constants are tabulated in Table 2.

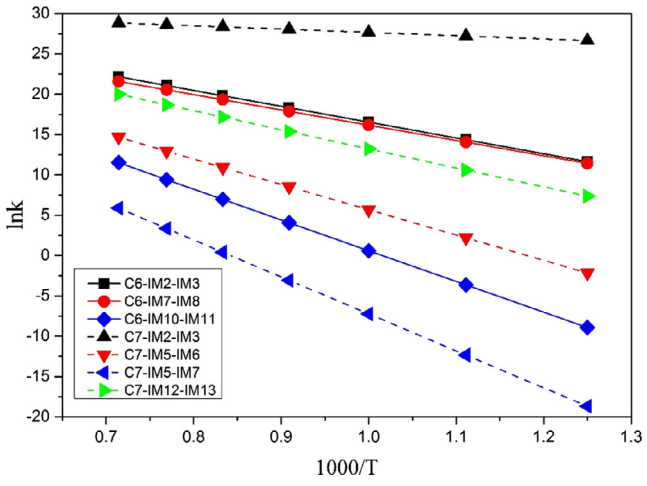

Fig. 6. Reaction rate constants for rate-determining steps.

From Fig. 6, reaction rate constants increase with the increase of temperature, revealing that heterogeneous reduction of N_2O by char is largely affected by the temperature which is consistent with experimental results that a higher combustion temperature contributes to lower N_2O emission [12,16]. Rate constants of oxygen desorption are lower than N_2 desorption, because activation energy of oxygen desorption is higher than N_2 desorption in general, as shown in Table 2. Rate constant of N_2 desorption from zigzag char edge is greatest, which is in agreement with the smallest activation energy (33.91 kJ/mol).

Comparing activation energy values of oxygen desorption with CO and without CO, activation energy of oxygen desorption with CO is much lower than that without CO, revealing that CO can reduce reaction energy barrier. From the microscopic reaction process and kinetics calculation results, Wang et al. [12] experimental phenomena can be well explained in molecular level and the heterogeneous reduction mechanism of N_2O by char is deepened in further. In addition, the promotion effect of CO on N_2O reduction is consistent with theoretical calculation results on other catalyzer [9].

Furthermore, for activation energy of homogeneous reaction between N_2O and CO, experimental and theoretical results are 184.10 and 277.82 kJ/mol respectively which are higher than N_2O decomposition on char edge [17,39], revealing that char edge can not only provide reaction location but also reduce the reaction energy barrier.

In Table 2, activation energy of N_2O decomposition on zigzag char edge is lower than armchair char edge (33.91 kJ/mol vs 163.58 kJ/mol), which is mainly due to the activity of free sites on char edge. Previous theoretical study indicated that zigzag char

Table 2
Kinetic parameters for rate-determining steps.

Char edge	Stages	Reaction steps	Pre-exponential factor *A*	Activation energy Ea (kJ·mol^{-1})	Arrhenius equations
Armchair	N_2O decomposition	IM2 → IM3	5.33×10^{15}	163.58	5.33×10^{15}exp (−19675.25/T)
	Oxygen desorption (CO)	IM7 → IM8	1.79×10^{15}	157.72	1.79×10^{15}exp (−18970.41/T)
	Oxygen desorption	IM10 → IM11	6.91×10^{16}	317.41	6.91×10^{16}exp (−38177.77/T)
Zigzag	N_2O decomposition	IM2 → IM3	6.10×10^{13}	33.91	6.10×10^{13}exp (−4078.66/T)
	Oxygen desorption (Spin = 2)	IM5 → IM6	1.30×10^{16}	261.23	1.30×10^{16}exp (−31420.50/T)
	Oxygen desorption(Spin = 4)	IM5 → IM8	5.95×10^{16}	381.29	5.95×10^{16}exp (−45861.20/T)
	Oxygen desorption (CO)	IM12 → IM13	1.02×10^{16}	196.44	1.02×10^{16}exp (−23627.62/T)

edge has higher reaction activity compared with armchair [23,40], so similar reaction processes on the two kinds of char edges are significantly different in activation energy value. Furthermore, activation energy of N_2O decomposition on char edge is about at the range of 66–115 kJ/mol in precious experimental research [16], while the calculation results in the current study are 33.91 and 163.58 kJ/mol. In practical coal combustion environment, two kinds of char edge models exist at different proportion and their comprehensive apparent activation energy magnitude could be consistent with the experimental results. Therefore, in order to acquire accurate calculation results, different calculation models should be taken into account, especially in the investigation of N_2O heterogeneous reduction by char.

4. Conclusion

Reaction pathways, thermodynamic and kinetics calculation have been performed in the present work to investigate the heterogeneous reduction of N_2O by char via density functional theory. Stemming from the above calculated results and discussion, five conclusions can be conclude by the following:

(1) Heterogeneous reduction of N_2O by char undergoes two stages, N_2O decomposition on char edge and residual oxygen desorption from char edge. N_2O decomposition on the two kinds of char edges experiences similar reaction process, while oxygen desorption from the two kinds of char edges accomplishes via obviously different paths.
(2) N_2O decomposition process is an exothermic reaction and takes place spontaneously and irreversibly at the operating temperature of circulating fluidized bed.
(3) In the presence of CO, char acts as an important catalyst which not only provides free sites as reaction location but also reduce the reaction energy barrier. In the absence of CO, char reacts with residual oxygen absorbed on char edge into CO molecule via a higher energy barrier.
(4) The participation of CO can significantly reduce reaction activation energy of residual oxygen desorption and promote reaction rate of heterogeneous reduction of N_2O by char.
(5) Char edge structure has notable influence on activation energy of N_2O decomposition on char edge. Activation energy values of N_2O decomposition on zigzag and armchair char edge are 33.91 kJ/mol and 163.58 kJ/mol, respectively.

For further studies, it may be of interest to investigate the effect of CO and residual oxygen on N_2O decomposition stage. Gas concentration effect on competitive adsorption process should be investigated in order to improve this heterogeneous reduction mechanism. In addition, in light of diversity and complexity of char edge in real combustion process, similar theoretical calculations of the current study on defect char and char nitrogen should be performed to provide further insight into the detail mechanism of N_2O heterogeneous reduction by char.

Acknowledgement

This work was supported by the National Natural Science Foundation of China (No. 91545122) and the Fundamental Research Funds for the Central Universities (JB2015RCY03).

References

[1] C.J. Tullin, S. Goel, A. Morihara, et al., Nitrogen oxide (NO and N_2O) formation for coal combustion in a fluidized bed: effect of carbon conversion and bed temperature, Energy Fuels 7 (6) (1993) 796–802.
[2] M. De las Obras-Loscertales, T. Mendiara, A. Rufas, NO and N_2O emissions in oxy-fuel combustion of coal in a bubbling fluidized bed combustor, Fuel 150 (2015) 146–153.
[3] B.X. Shen, T. Mi, D.C. Liu, et al., N_2O emission under fluidized bed combustion condition, Fuel Process. Technol. 84 (1) (2003) 13–21.
[4] H. Liu, B.M. Gibbs, The influence of calcined limestone on NO_x and N_2O emissions from char combustion in fluidized bed combustors, Fuel 80 (9) (2001) 1211–1215.
[5] K. Svoboda, M. Pohořelý, Influence of operating conditions and coal properties on NO_x and N_2O emissions in pressurized fluidized bed combustion of subbituminous coals, Fuel 83 (7) (2004) 1095–1103.
[6] R. Amrousse, T. Katsumi, Substituted ferrite $M_xFe_{1-x}Fe_2O_4$ (M=Mn, Zn) catalysts for N_2O catalytic decomposition processes, Catal. Commun. 26 (2012) 194–198.
[7] L.G. Pinaeva, L.A. Isupova, I.P. Prosvirin, et al., La–Fe–O/CeO2 based composites as the catalysts for high temperature N_2O decomposition and CH_4 combustion, Catalysis letters 143 (12) (2013) 1294–1303.
[8] Z.M. Liu, F. He, L.L. Ma, et al., Recent advances in catalytic decomposition of N_2O on noble metal and metal oxide catalysts, Catal. Surv. Asia 20 (3) (2016) 121–132.
[9] C. Dai, Z. Lei, Y. Wang, et al., Reduction of N_2O by CO over Fe-and Cu-BEA zeolites: an experimental and computational study of the mechanism, Microporous and Mesoporous Mater. 167 (2013) 254–266.
[10] C.P. Cho, Y.D. Pyo, J.Y. Jang, et al., NO_X reduction and N_2O emissions in a diesel engine exhaust using Fe-zeolite and vanadium based SCR catalysts, Appl. Therm. Eng. 110 (2017) 18–24.
[11] S. Li, M. Xu, L. Jia, et al., Influence of operating parameters on N_2O emission in O_2/CO_2 combustion with high oxygen concentration in circulating fluidized bed, Appl. Energy 173 (2016) 197–209.
[12] C. Wang, Y. Du, D. Che, Study on N_2O reduction with synthetic coal char and high concentration CO during oxy-fuel combustion, Proc. Combust. Inst. 35 (2) (2015) 2323–2330.
[13] S.A. Carabineiro, L.S. Lobo, Understanding the reactions of CO_2, NO, and N_2O with activated carbon catalyzed by binary mixtures, Energy Fuels 30 (9) (2016) 6881–6891.
[14] L. Armesto, H. Boerrigter, A. Bahillo, et al., N_2O emissions from fluidised bed combustion. The effect of fuel characteristics and operating conditions, Fuel 82 (15) (2003) 1845–1850.
[15] K. Noda, P. Chambrion, T. Kyotani, et al., A study of the N_2 formation mechanism in carbon-N_2O reaction by using isotope gases, Energy & Fuels 13 (4) (1999) 941–946.
[16] Y.H. Li, G.Q. Lu, V. Rudolph, The kinetics of NO and N_2O reduction over coal chars in fluidized bed combustion, Chem. Eng. Sci. 53 (1) (1998) 1–26.
[17] P. Kilpinen, M. Hupa, Homogeneous N_2O chemistry at fluidized bed combustion conditions: A kinetic modeling study, Combust. Flame 85 (1–2) (1991) 94–104.
[18] T. Kyotani, A. Tomita, Analysis of the reaction of carbon with NO/N_2O using ab initio molecular orbital theory[J], J. Phys. Chem. B 103 (17) (1999) 3434–3441.
[19] A. Arenillas, B. Arias, F. Rubiera, et al., Heterogeneous reaction mechanisms of the reduction of nitric oxide on carbon surfaces: a theoretical analysis, Theoret. Chem. Acc. 127 (1–2) (2010) 95–108.
[20] X. Zhang, Z. Zhou, J. Zhou, et al., Analysis of the reaction between O_2 and nitrogen-containing char using the density functional theory, Energy Fuels 25 (2) (2011) 670–675.
[21] H. Zhang, J. Liu, J. Shen, et al., Thermodynamic and kinetic evaluation of the reaction between NO (nitric oxide) and char (N)(char bound nitrogen) in coal combustion, Energy 82 (2015) 312–321.

[22] S.T. Perry, E.M. Hambly, T.H. Fletcher, et al., Solid-state ^{13}C NMR characterization of matched tars and chars from rapid coal devolatilization, Proc. Combust. Inst. 28 (2) (2000) 2313–2319.
[23] N. Chen, R.T. Yang, Ab initio molecular orbital calculation on graphite: Selection of molecular system and model chemistry, Carbon 36 (7) (1998) 1061–1070.
[24] F.H. Yang, R.T. Yang, Ab initio molecular orbital study of adsorption of atomic hydrogen on graphite: Insight into hydrogen storage in carbon nanotubes, Carbon 40 (3) (2002) 437–444.
[25] N. Chen, R.T. Yang, Ab initio molecular orbital study of the unified mechanism and pathways for gas-carbon reactions, The Journal of Physical Chemistry A 102 (31) (1998) 6348–6356.
[26] X. Zhang, Z. Zhou, J. Zhou, et al., Density functional study of NO desorption from oxidation of nitrogen containing char by O_2, Combust. Sci. Technol. 184 (4) (2012) 445–455.
[27] P. He, X. Zhang, X. Peng, et al., Interaction of elemental mercury with defective carbonaceous cluster, J. Hazard. Mater. 300 (2015) 289–297.
[28] Z.H. Zhu, J. Finnerty, G.Q. Lu, et al., A comparative study of carbon gasification with O_2 and CO_2 by density functional theory calculations, Energy & Fuels 16 (6) (2002) 1359–1368.
[29] Z.H. Zhu, J. Finnerty, G.Q. Lu, et al., Molecular orbital theory calculations of the H_2O-carbon reaction, Energy & fuels 16 (4) (2002) 847–854.
[30] K. Sendt, B.S. Haynes, Density functional study of the chemisorption of O_2 on the zigzag surface of graphite, Combustion and flame 143 (4) (2005) 629–643.
[31] K. Sendt, B.S. Haynes, Density functional study of the chemisorption of O_2 across two rings of the armchair surface of graphite, J. Phys. Chem. C 111 (14) (2007) 5465–5473.
[32] J. Liu, W. Qu, J. Yuan, et al., Theoretical studies of properties and reactions involving mercury species present in combustion flue gases, Energy Fuels 24 (1) (2009) 117–122.
[33] M. J. Frisch, G. W. Trucks, et al. Gaussian 09, Revision D.01; Gaussian, Inc., Wallingford CT, 2009.
[34] G. Bravoperez, J.R. Alvarezidaboy, A. Cruztorres, et al., Quantum chemical and conventional transition-state theory calculations of rate constants for the NO_3+alkane reaction, J. Phys. Chem. A 106 (18) (2002) 4645–4650.
[35] P.A. Korevaar, S.J. George, A.J. Markvoort, et al., Pathway complexity in supramolecular polymerization, Nature 481 (7382) (2012) 492–496.
[36] M. Noei, DFT study on the sensitivity of open edge graphene toward CO_2 gas, Vacuum 131 (2016) 194–200.
[37] L.R. Radovic, The mechanism of CO_2 chemisorption on zigzag carbon active sites: a computational chemistry study, Carbon 43 (5) (2005) 907–915.
[38] B. Padak, J. Wilcox, Understanding mercury binding on activated carbon, Carbon 47 (12) (2009) 2855–2864.
[39] Y. Wang, G. Fu, Y. Zhang, et al., O-atom transfer reaction from N_2O to CO: A theoretical investigation, Chem. Phys. Lett. 475 (4) (2009) 202–207.
[40] L.R. Radovic, B. Bockrath, On the chemical nature of graphene edges: origin of stability and potential for magnetism in carbon materials, J. Am. Chem. Soc. 127 (16) (2005) 5917–5927.